



EXPLOITING NONLINEARITIES AND CHAOS TO ENHANCE ENERGY HARVESTING SYSTEM USING PIEZOELECTRIC DEVICES

Cláudio Henrique Cerqueira Costa Basquerotto
Fábio Roberto Chavarette
Samuel da Silva

UNESP - Univ Estadual Paulista, Faculdade de Engenharia de Ilha Solteira, Departamento de Engenharia Mecânica
cbasquerotto@gmail.com; fabioch@mat.feis.unesp.br; samuel@dem.feis.unesp.br

Abstract. *The use of piezoelectric devices for energy harvesting through mechanical vibration has been increasing in the last years. This concept is particularly important for systems remotely operated and with limited sources of energy, for example in structural health monitoring systems in areas of difficult access. In general, the common approaches for energy harvesting have been employing linear systems. However, they are limited for applications where excitations are close to the resonant frequency of the system. If the objective is to work with a frequency broad bandwidth, when vibration source is not single, nonlinear oscillators can present better performance. Thus, this paper shows a nonlinear piezoelectric harvester that can operate with chaotic behavior. The Lyapunov exponents are computed by method of Wolf in order to check if the nonlinear system is chaotic. Similarly, it is useful to classify whether the system is chaotic, as well as to identify the forms in which this behavior may change. The bifurcation plot has been implemented to illustrate the qualitative change in the systems solution form. Several numerical tests are performed and the results show the advantage and drawbacks of the energy harvesting system.*

Keywords: *Energy Harvesting, Duffing oscillator, chaos, Lyapunov exponents, bifurcation diagram.*

1. INTRODUCTION

The idea of harvesting ambient mechanical vibration energy to generate electricity have received much attention over the past few years due to reduced power requirements of small electronic components. The three basic mechanisms for converting vibrations into electricity are: piezoelectric (Roundy *et al.*, 2003; Sodano *et al.*, 2004 ; Erturk *et al.*, 2010); electromagnetic (Williams and Yates, 1996; Mitcherson *et al.*, 2004); and electrostatic (Erturk *et al.*, 2010). The piezoelectric transduction has received the most attention, as evidenced by several publications using this type of mechanism.

Linear devices have been the most common type of generator used in harvesting energy. However, good performance of generation is limited to a narrow frequency band thus the device is optimally tuned so that its natural frequency coincides with the excitation frequency (Ramlan *et al.*, 2010). In order to overcome the bandwidth issue of the conventional cantilever configuration, researchers have considered to utilize nonlinear dynamical systems (Erturk *et al.*, 2010).

The nonlinear structure that forms the basis of this work was first investigated by Moon and Holmes (1979) as a mechanical structure that exhibits strange attractor motions. Erturk *et al.* (2009) investigated a nonlinear mechanism of broadband proposed by Moon and Holmes (1979) under sinusoidal excitations. Erturk *et al.* (2010) investigated the broadband high-energy orbits in a nonlinear energy harvester device along with a critique of the possible advantage of the chaotic response over the conventional periodic response. Litak *et al.* (2012) studied an energy harvesting system of two magnetopiezoelectric oscillators coupled by electric circuit and driven by harmonic excitation, focusing on the effects of synchronization and escape from a single potential well.

The main goal of this work is to show the use of a nonlinear system for energy harvesting. This paper describes a nonlinear mechanism for energy harvesting devices. The first step shows the performance of a non-linear device by comparing with a linear system for energy harvesting. Through the analysis of the first stage results, one can see that the nonlinear system can be chaotic. To demonstrate the chaotic behavior the Lyapunov exponents are computed by the method of Wolf. It is also useful to classify the behavior of a system by identifying the forms in which this behavior can be changed. In order to show these changes the bifurcation plots were implemented. Several numerical tests are performed and the results show the advantage and drawback of the energy harvesting system.

This paper is organized into five sections. The next section presents a linear energy harvesting device. In the following, a nonlinear energy harvesting device is shown. After, the results are presented and discussed. Finally, the concluding remarks are shown followed by suggestions for future works.

2. LINEAR ENERGY HARVESTING DEVICE

The linear energy harvesting device (Fig. 1(a)) consists of a ferromagnetic cantilever attached to piezoceramic layers to obtain a bi-morph generator. The piezoceramic layers are connected to an electrical load (a resistor for simplicity) and

the output voltage of the generator across the loads monitored. The motion equation is described by (Erturk *et al.*, 2010; Erturk and Inman, 2011a; Erturk and Inman, 2011b):

$$\ddot{x} + 2\zeta\dot{x} + x - \chi v = f \cos \Omega t \quad (1)$$

$$\dot{v} + \Lambda v + \kappa \dot{x} = 0 \quad (2)$$

where x is the dimensionless tip displacement of the ferromagnetic cantilever, ζ is the mechanical damping ratio, Ω is the dimensionless excitation frequency, f is the dimensionless excitation force due to base acceleration, v is the dimensionless voltage across the load resistance, χ is the dimensionless piezoelectric coupling term in the mechanical equation, κ is the dimensionless piezoelectric coupling term in the electrical circuit equation and Λ is the reciprocal of the dimensionless time constant ($\Lambda \propto 1/R_l C_p$ where R_l is the load resistance and C_p is the equivalent capacitance of the piezoceramic layers).

Defining the states $u_1 = x$, $u_2 = \dot{x}$ and $u_3 = v$ it follows:

$$\begin{Bmatrix} \dot{u}_1 \\ \dot{u}_2 \\ \dot{u}_3 \end{Bmatrix} = \begin{bmatrix} 0 & 1 & 0 \\ -1 & -2\zeta & \chi \\ 0 & -\kappa & -\Lambda \end{bmatrix} \begin{Bmatrix} u_1 \\ u_2 \\ u_3 \end{Bmatrix} + \begin{bmatrix} 0 \\ 1 \\ 0 \end{bmatrix} f \cos \Omega t \implies \dot{\mathbf{u}} = \mathbf{A}\mathbf{u} + \mathbf{B}f \cos \Omega t \quad (3)$$

where \mathbf{A} is the dynamic matrix and \mathbf{B} is the input matrix. The potential energy V of the system can be computed by:

$$V = \frac{1}{2}x^2 \quad (4)$$

These systems have only an appreciable amplitude response if the vibration frequency is close to the devices natural frequency. For one aspect of vibration broadband connection that is found in the environment in real cases, only a fraction of the available energy of the vibration can be extracted by these devices. When working with a frequency bandwidth broader, when the vibration source is broadband, nonlinear oscillators may show better performance (Chen *et al.*, 2010).

3. NONLINEAR ENERGY HARVESTING DEVICE

The nonlinear energy harvesting device consists of a ferromagnetic cantilever with two permanent magnets located symmetrically near to the end free end excited by harmonic base force. Depending on the magnet spacing, the ferromagnetic beam may have five or three equilibrium positions with three or two stable positions, respectively, or only one stable position.

In order to use this device as a piezoelectric energy harvester, two piezoelectric layers (Figure 1) are connected to an electrical load (a resistor for simplicity). The generators output voltage across the load due to seismic excitation is the primary interest in energy harvesting. The fundamental vibration equations that describe the systems dynamics for the three equilibrium positions case are defined as (Erturk *et al.*, 2010; Erturk and Inman, 2011a; Erturk and Inman, 2011b):

$$\ddot{x} + 2\zeta\dot{x} - \frac{1}{2}x(1 - x^2) - \chi v = f \cos \Omega t \quad (5)$$

$$\dot{v} + \Lambda v + \kappa \dot{x} = 0 \quad (6)$$

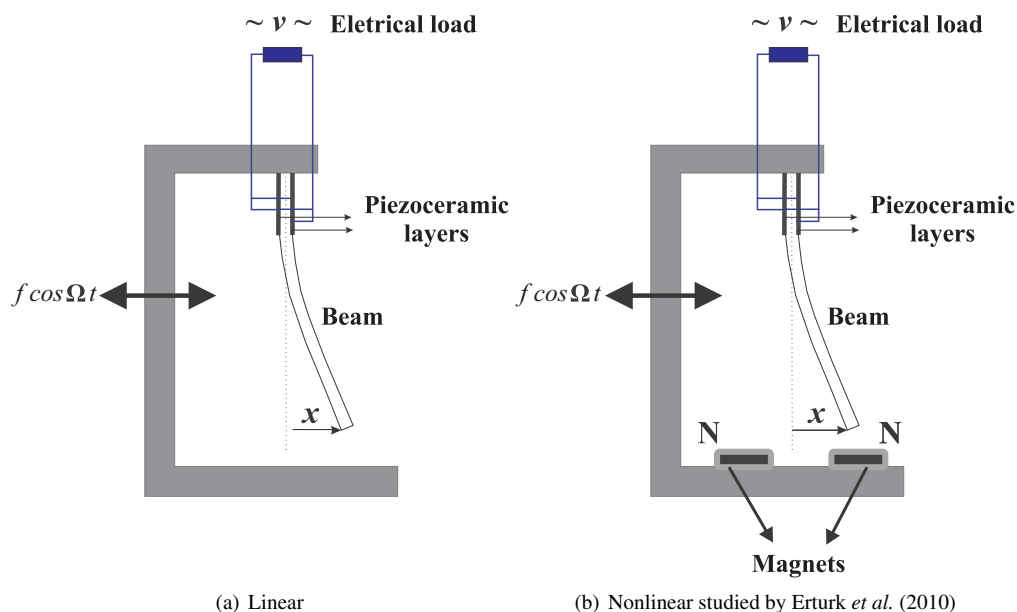


Figure 1. Energy harvesting devices.

The state-space model can be obtained by:

$$\begin{cases} \dot{u}_1 \\ \dot{u}_2 \\ \dot{u}_3 \end{cases} = \begin{cases} u_2 \\ -2\zeta u_2 + \frac{1}{2}u_1(1 - u_1^2) + \chi u_3 + f \cos \Omega t \\ -\Lambda u_3 - \kappa u_2 \end{cases} \quad (7)$$

The potential energy (V) of the system is given by:

$$V = -\frac{1}{2}x^2 + \frac{1}{2}x^4 \quad (8)$$

when the three static equilibrium positions are $(x, \dot{x}) = (0,0)$ (a saddle) and $(x, \dot{x}) = (\pm 1, 0)$ (two sinks).

4. RESULTS

This section presents the analytical results used to illustrate the methods studied in this work. The examples are made based on simulations and experimental data from the literature (Erturk *et al.*, 2010; Erturk and Inman, 2011a; Erturk and Inman, 2011b). The goal is to compare the performance of linear and nonlinear energy harvesting devices. The iterative method of Runge-Kutta was used to solve ordinary differential equations.

The values used for parameters of both linear and nonlinear energy harvesting presented in Table 1 are used by (Erturk *et al.*, 2010; Erturk and Inman, 2011a) for generating better energy extraction from vibrational motion.

Table 1. Parameters of the reference model.

Parameters	Values
Ω	0.8
ζ	0.01
χ	0.05
κ	0.5
Λ	0.05
f	0.083

All tests used samples ranging from 0-2500 with a step of 0.1. The time-domain voltage tests are shown in Figures (2) and (3). It may be noted that the response of the nonlinear device has a much greater extent when compared to the linear device.

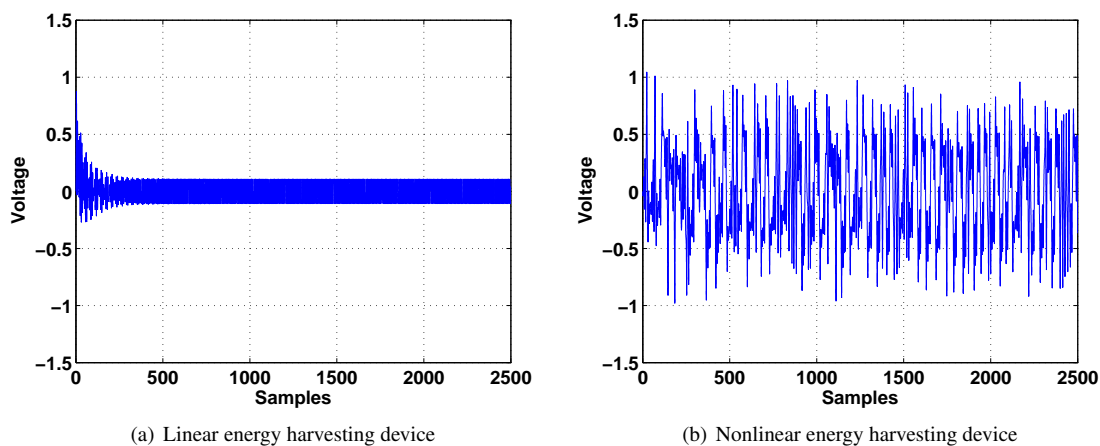


Figure 2. Time domain voltage.

If the excitation amplitude is increased while maintaining the same initial conditions, the chaotic behavior is followed by transient fluctuations over a wide range of high energy orbit (Figure 3). Observing Figure (3b), it is worthy to note that one can obtain a large voltage amplitude with the same force amplitude and different initial conditions ($x(0)=1$, $\dot{x}(0)=1.2$ and $v(0)=0$).

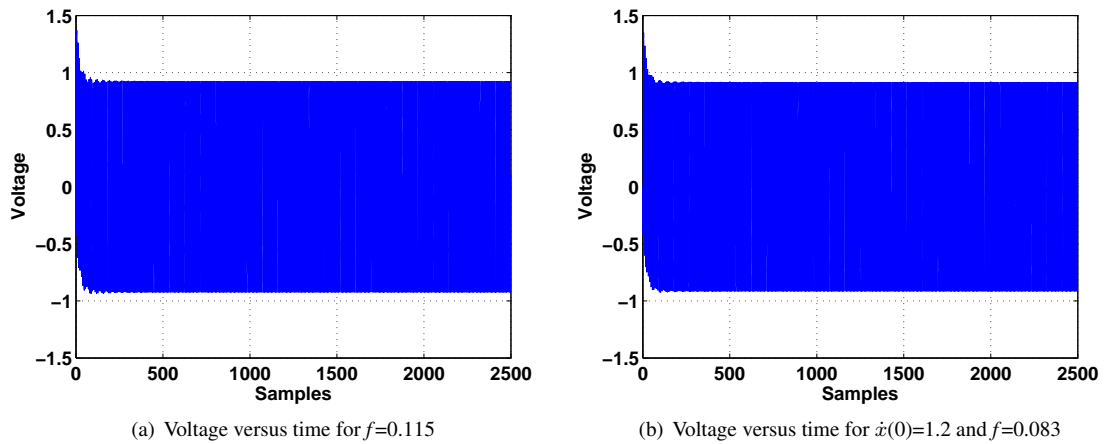


Figure 3. Time domain voltage for the nonlinear energy harvesting device.

Figure (4a) shows the phase portrait of the velocity as a function of displacement comparing the linear and nonlinear energy harvesting device. It is observed from the state that vibration amplitude of the non-linear device can be much higher than the linear device for the same amplitude force. Likewise, Figure (4b) shows the velocity as a function of the voltage in phase portrait, which is also higher for the nonlinear system. It can be seen in Figure (5) that the excitation frequency change kept the nonlinear systems voltage greater than the linear systems voltage.

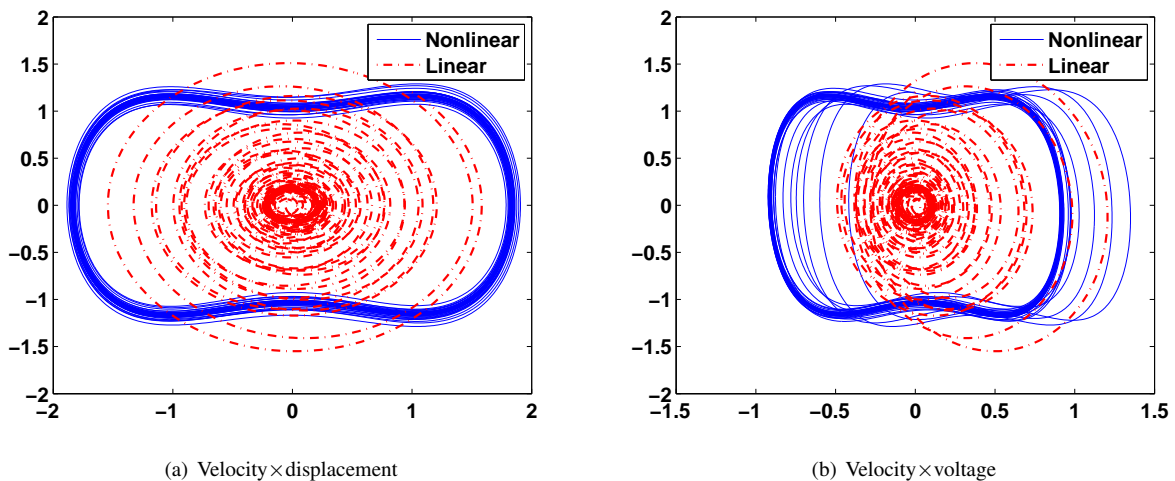


Figure 4. Phase portrait for linear and non-linear configurations ($x(0)=1$, $\dot{x}(0)=1.2$, $v=0$, $\Omega=0.8$ and $f=0.083$).

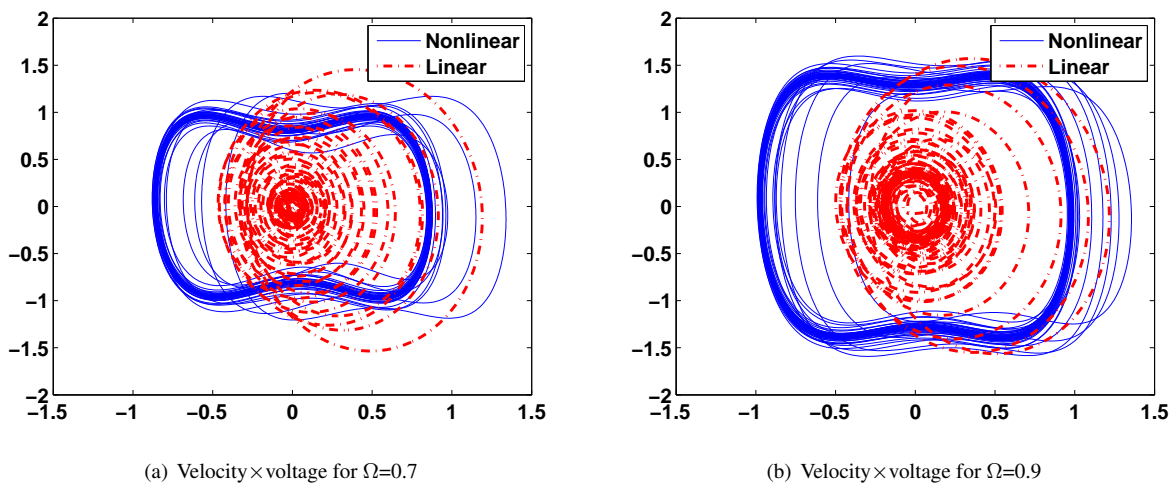


Figure 5. Comparing the speed and voltage systems linear and nonlinear ($x(0)=1$, $\dot{x}(0)=1.2$, $v=0$ and $f=0.083$).

After concluding that the nonlinear energy harvesting device is best for energy harvesting frequency broadband compared to the linear system, the next step analysed the nonlinear dynamics of the nonlinear energy harvesting device requiring a linearization procedure. The linearization of a dynamic system around a known solution is a mode information for the dynamics of a system to uniquely evaluate the stability of the solution (Savi, 2006).

To linearize the system, the Jacobian is applied in the state-space model of the nonlinear device (Equation 9):

$$J(u_1, u_2, u_3) = \begin{bmatrix} \frac{\partial}{\partial y^1} & \frac{\partial}{\partial y^2} & \frac{\partial}{\partial y^3} \\ \frac{\partial}{\partial u^1} & \frac{\partial}{\partial u^2} & \frac{\partial}{\partial u^3} \end{bmatrix} \rightarrow J = \begin{bmatrix} 0 & 1 & 0 \\ -\frac{1}{2} - \frac{3u_1^2}{2} & -2\zeta & \chi \\ 0 & -\kappa & -\Lambda \end{bmatrix} \quad (9)$$

The potential energy was computed followed by the observation of the existence of two points of stability when the offset is -1 and 1 besides a point of stability for the offset equal to zero. One way to classify the equilibrium point of a system is by calculating its eigenvalues. If all eigenvalues have negative real part, then it is concluded that this point is asymptotically stable. The following expression gives the eigenvalues of the nonlinear energy harvesting device:

$$\gamma = \{-0.0105 + 1.1210i; -0.0105 - 1.1210i; -0.0490\} \quad (10)$$

where i is the imaginary term. Figure (6) shows the potential energy \times displacement with equilibrium points.

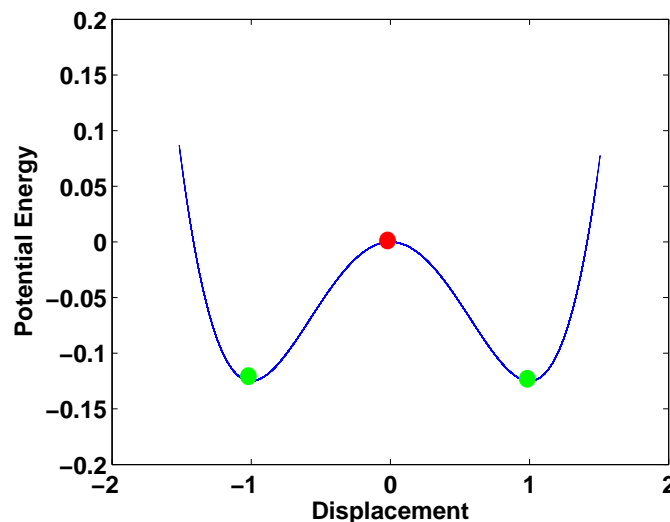


Figure 6. Potential energy with the equilibrium positions for the nonlinear energy harvesting device.

Next, the method of Wolf was used to compute the Lyapunov exponents for certain amplitude values as shown in Table 2:

Table 2. Values of the amplitude of excitation.

Values of f	0.053	0.063	0.073	0.083	0.093	0.103	0.113	0.123	0.133
---------------	-------	-------	-------	-------	-------	-------	-------	-------	-------

By analysing the values of Lyapunov exponents (Figures 7 and 10), it can be seen that the system is chaotic for certain values of the excitation amplitude and frequency. For a range of amplitude values between 0.063 and 0.123 and frequency between 0.8 and 1.0 the system is in chaos, for other values outside this range, the system is not chaotic.

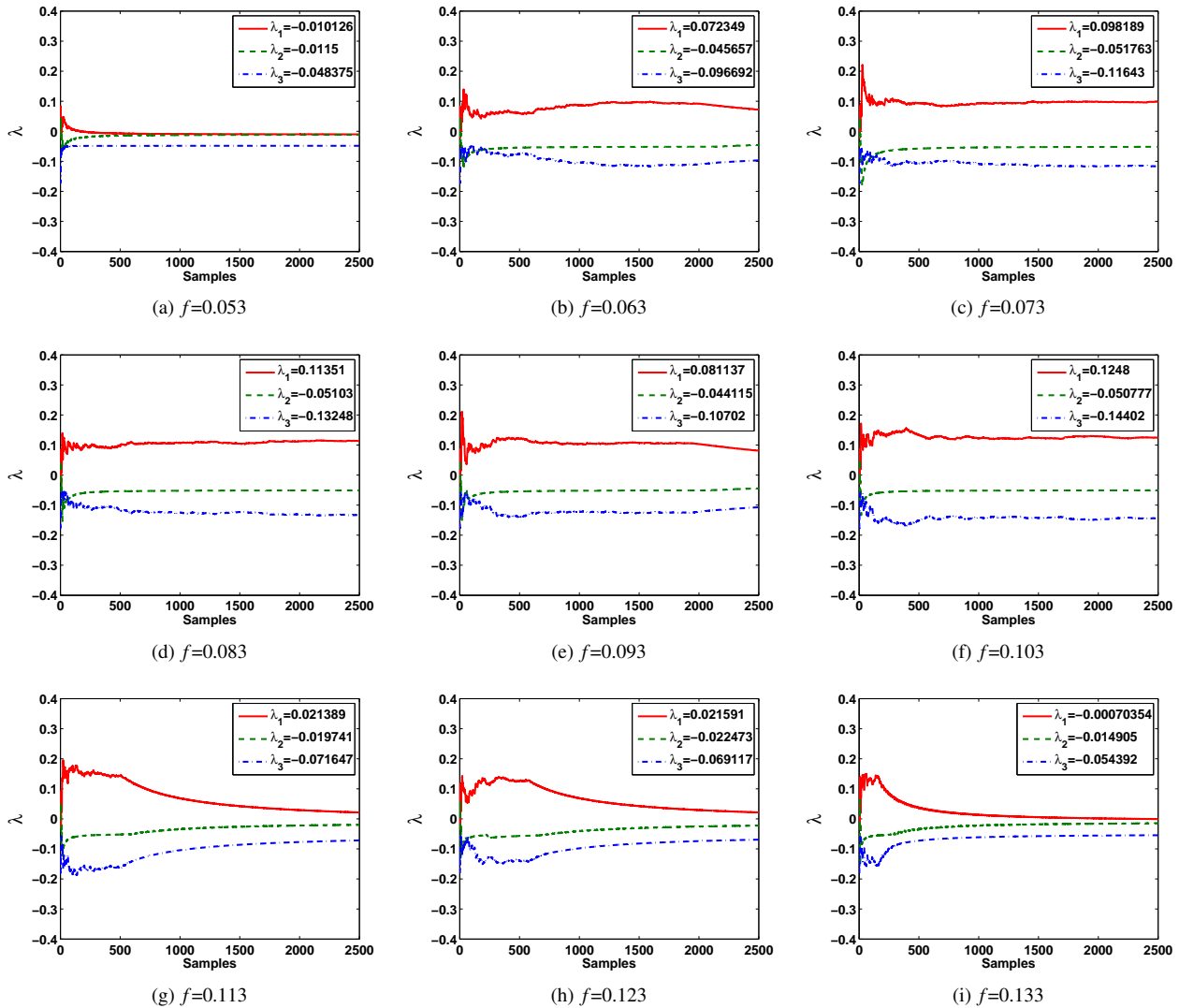
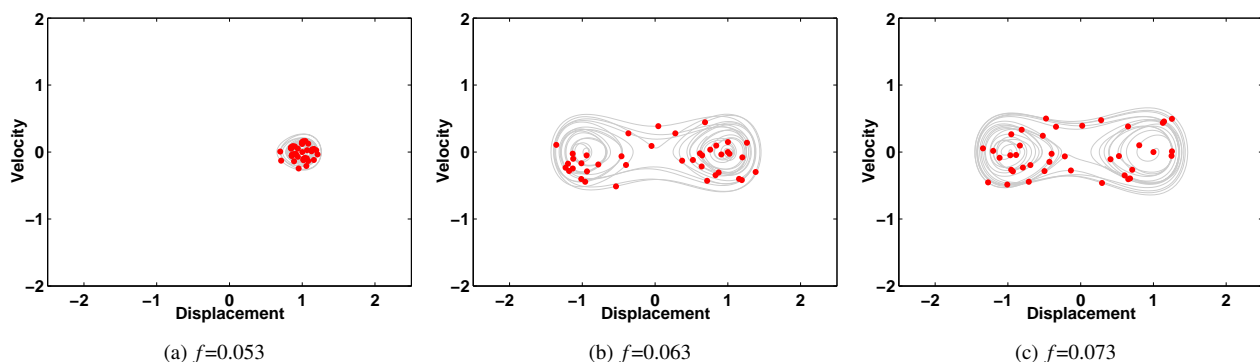


Figure 7. Lyapunov exponents calculated by the method of Wolf.

A very important tool in a temporal analysis was developed by Henry Poincaré, called Poincaré mapping. It shows the flow of the solution in the phase portrait. The number of points in the Poincaré map of the permanent solution of a forced system shows the frequency response. When the points on the map of Poincaré repeats, they are called fixed points and the response is periodic, when there is an infinite number of them, the answer may be chaotic or quasi-periodic. As can be seen in Figure (8), there are a large number of points indicating that the system is chaos for f ranging 0.063 to 0.123 and for Ω ranging 0.7 to 0.9 (Figure 11).



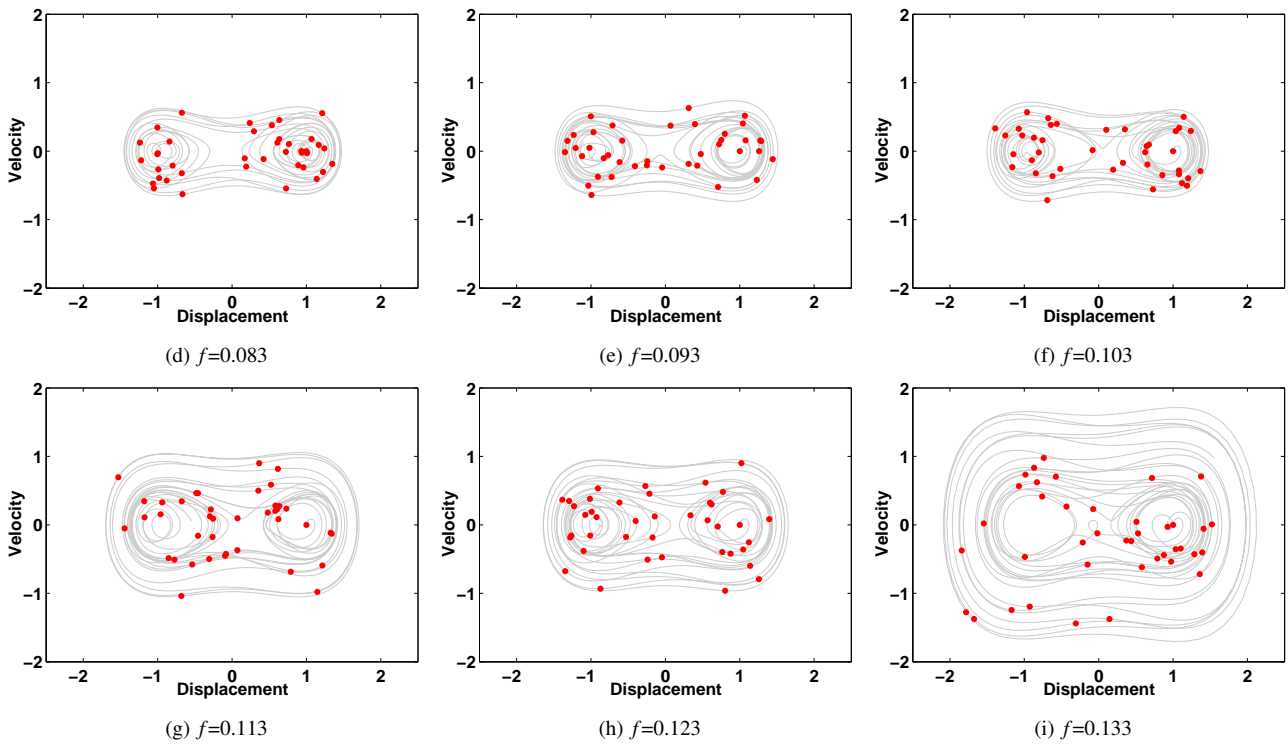


Figure 8. Phase portrait with Poincaré's map.

The bifurcation plots of nonlinear energy devices are shown in Figures (9) and (12) which show that for certain values of f and Ω the systems displacement and voltage change greatly. When f varies from 0 to 0.053 and Ω varies from 0 to 0.7, the system is stable. The points $f=0.063$ e $\Omega=0.7$ are associated with a bifurcation point where the line splits in two thus replacing the stable fixed point. This sequence of bifurcations continues featuring a cascade of doubling periods culminating in the emergence of chaos, characterized by a cloud of points in the diagram.

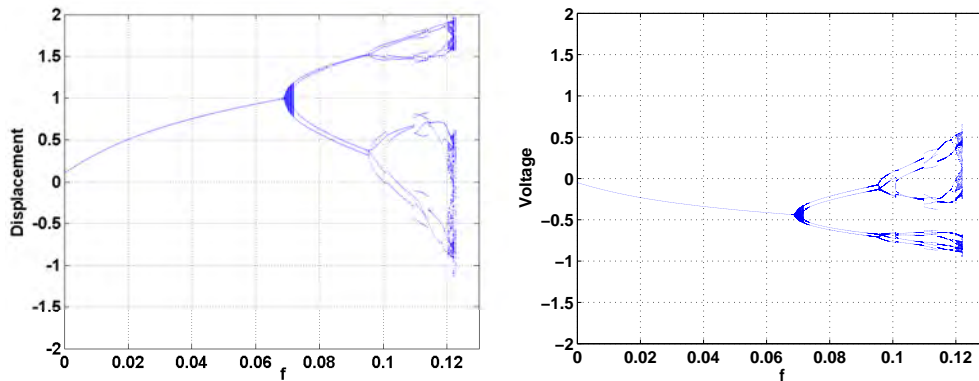


Figure 9. Bifurcation diagram.

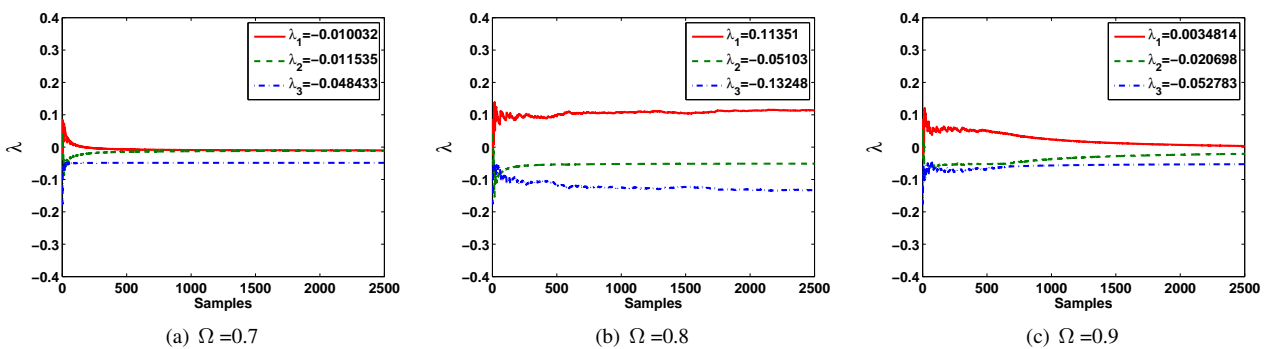


Figure 10. Lyapunov exponents calculated by the method of Wolf.

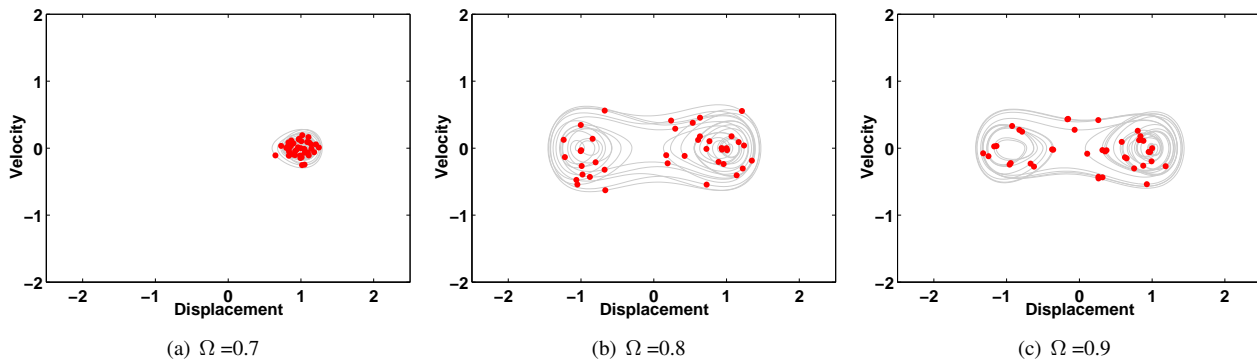


Figure 11. Phase portrait with Poincaré's map.

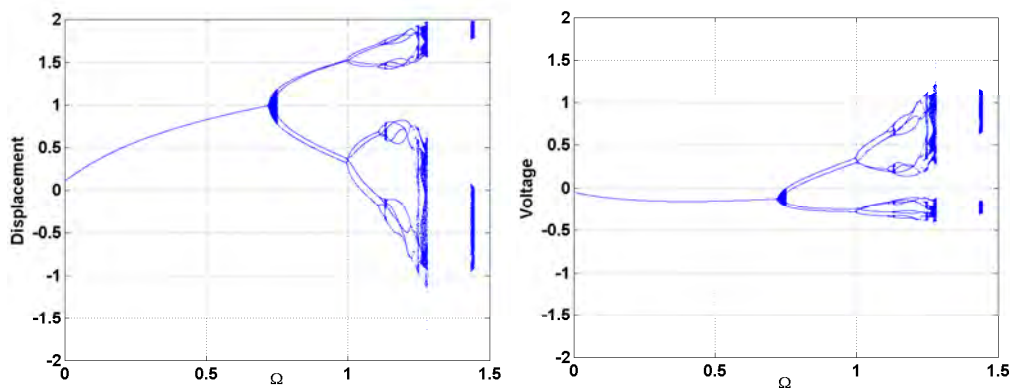


Figure 12. Bifurcation diagram.

5. FINAL REMARKS

The extraction of energy from vibrational motion has received much attention in the last decade. This paper presented two devices for energy harvesting: one linear and the other nonlinear. Tests show that the nonlinear device has orbits of higher energy than the linear device. The literature in the energy harvesting states that the nonlinear system studied in this work is in fact nonlinear without proving this fact. The novelty of this work is the proof of the devices chaotic behavior which is still not available in the literature to the present date. This work has shown through testing that the nonlinear energy harvesting device is chaotic for certain values of Ω and f . The results show that the chaotic behavior need to be well synchronized to obtain large values of energy extracted. So, the author point out that it could be difficult to obtain a practical situation for this condition. Another point that need to be addressed is associated to the requirement to work with direct current. In this sense, it is fundamental to consider together a rectifier circuit.

6. ACKNOWLEDGEMENTS

The authors acknowledge the financial support provided by Research Foundation of São Paulo (FAPESP) by grant number 12/09135-3 and National Council for Scientific and Technological Development (CNPq) grant number 470582/2012-0. The authors also would like to thank to CNPq and Minas Gerais State Research Foundation (FAPEMIG) for funding through the National Institute of Science and Technology in Smart Structures (INCT-EIE). The first author would like to thank the CAPES for his scholarship.

7. REFERENCES

- Chen, Y.Y., Vasic, D., Costa, F. and Wu, W., 2010. "Nonlinear magnetic coupling of a piezoelectric energy harvesting cantilever combined with velocity-controlled synchronized switching technique". *Power MEMS*.
- Erturk, A., Hoffmann, J. and Inman, D., 2009. "A piezomagnetoelastic structure for broadband vibration energy harvesting". *Applied Physics Letters*, Vol. 94, No. 25, pp. 254102–254102–3. ISSN 0003-6951. doi:10.1063/1.3159815.
- Erturk, A. and Inman, D., 2011a. "Broadband piezoelectric power generation on high-energy orbits of the bistable duffing oscillator with electromechanical coupling". *Journal of Sound and Vibration*, Vol. 330, No. 10, pp. 2339 – 2353. ISSN 0022-460X. doi:10.1016/j.jsv.2010.11.018. URL

22nd International Congress of Mechanical Engineering (COBEM 2013)
November 3-7, 2013, Ribeirão Preto, SP, Brazil

<http://www.sciencedirect.com/science/article/pii/S0022460X10007807>. <ce:title>Dynamics of Vibro-Impact Systems</ce:title>.

Erturk, A. and Inman, D., 2011b. *Piezoelectric Energy Harvesting*. Wiley.

Erturk, A., Vieira, W., De Marqui, C. and Inman, D., 2010. “On the energy harvesting potential of piezoaeroelastic systems”. *Applied Physics Letters*, Vol. 96, No. 18, p. 184103.

Litak, G., Friswell, M.I., Kwiimy, C.A.K., Adhikari, S. and Borowiec, M., 2012. “Energy harvesting by two magnetopiezoelastic oscillators with mistuning”. *Theoretical and Applied Mechanics Letters*, Vol. 2, No. 4, pp. 043009–043009.

Mitcheson, P., Miao, P., Stark, B., Yeatman, E., Holmes, A. and Green, T., 2004. “Mems electrostatic micropower generator for low frequency operation”. *Sensors and Actuators A: Physical*, Vol. 115, No. 23, pp. 523 – 529. ISSN 0924-4247. doi:10.1016/j.sna.2004.04.026. URL <http://www.sciencedirect.com/science/article/pii/S0924424704002985>. <ce:title>The 17th European Conference on Solid-State Transducers</ce:title>.

Moon, F. and Holmes, P., 1979. “A magnetoelastic strange attractor”. *Journal of Sound and Vibration*, Vol. 65, No. 2, pp. 275 – 296. ISSN 0022-460X. doi:10.1016/0022-460X(79)90520-0. URL <http://www.sciencedirect.com/science/article/pii/0022460X79905200>.

Ramlan, R., Brennan, M., Mace, B. and Kovacic, I., 2010. “Potential benefits of a non-linear stiffness in an energy harvesting device”. *Nonlinear dynamics*, Vol. 59, No. 4, pp. 545–558.

Roundy, S., Wright, P.K. and Rabaey, J., 2003. “A study of low level vibrations as a power source for wireless sensor nodes”. *Computer Communications*, Vol. 26, No. 11, pp. 1131 – 1144. ISSN 0140-3664. doi:10.1016/S0140-3664(02)00248-7. URL <http://www.sciencedirect.com/science/article/pii/S0140366402002487>. <ce:title>Ubiquitous Computing</ce:title>.

Savi, M.A., 2006. *Dinâmica não-linear e caos*. Editora E-papers.

Sodano, H.A., Inman, D.J. and Park, G., 2004. “A review of power harvesting from vibration using piezoelectric materials”. *Shock and Vibration Digest*, Vol. 36, No. 3, pp. 197–206.

Williams, C. and Yates, R., 1996. “Analysis of a micro-electric generator for microsystems”. *Sensors and Actuators A: Physical*, Vol. 52, No. 13, pp. 8 – 11. ISSN 0924-4247. doi:10.1016/0924-4247(96)80118-X. URL <http://www.sciencedirect.com/science/article/pii/092442479680118X>. <ce:title>Proceedings of the 8th International Conference on Solid-State Sensors and Actuators Eurosensors IX</ce:title>.

Wolf, A., Swift, J.B., Swinney, H.L. and Vastano, J.A., 1985. “Determining lyapunov exponents from a time series”. *Physica D: Nonlinear Phenomena*, Vol. 16, No. 3, pp. 285–317.

8. RESPONSIBILITY NOTICE

The authors are the only responsible for the printed material included in this paper.